Geotechnical Engineering Journal of the SEAGS & AGSSEA Vol. 45 No.4 December 2014 ISSN 0046-5828

Centrifuge Modelling of the Seismic Responses of a Gently Sloped Liquefiable Sand Deposit Confined within Parallel Walls

C.J. Lee[1], W.Y. Chung[2], and W.Y. Hung[3]
Department of Civil Engineering, National Central University, Jhongli City, Taiwan
E-mail: cjleeciv@ncu.edu.tw

ABSTRACT: A series of one-dimensional (1-*D*) centrifuge shaking table tests was performed to investigate the seismic responses of a 4° sloped liquefiable sand deposit confined within parallel walls, having various penetration depths and row distances, and with different fixed ends. The parallel walls relieved the build-up of excess pore water pressure in the deeper enclosed sand layer, but no obvious reductions were observed in the excess pore water pressure in the shallower sand layer during large earthquakes. The effective relief of the excess pore water pressure and decrease in the surface settlement within the walls would be expected to improve at deeper penetration depths and for higher wall bending stiffness values. Stiffer parallel walls with fixed ends can constrain the enclosed sands more effectively and prevent lateral displacement induced by lateral spreading occurred in gently sloped ground. The walls can also transmit larger accelerations into the enclosed soils. Protected structures would not, therefore, come in contact with the parallel walls, thereby avoiding experiencing larger accelerations.

KEYWORDS: Parallel walls, Liquefaction, Lateral spreading, Centrifuge modeling, Shaking table test.

1. INTRODUCTION

Loose saturated sands are susceptible to large excess pore water pressure generation during earthquakes, leading to a loss in the sand stiffness and strength. Investigations into damage sites after earthquakes reveal that soil liquefaction is one of the major factors that contribute to severe damage to buildings, oil tanks, bridges, tunnels, embankments, buried pipelines, and marine structures [Adalier et al. (2003); Abdoun et al. (2005); Dashti et al. (2010); Ishihara et al. (1996); Lee (2005)]. Permanent lateral ground displacements due to lateral spreading in a free field provide a main source of distress to piles. The effects of lateral spreading on pile foundations are very damaging and costly. The risk of seismically induced liquefaction and the associated ground deformations (i.e., surface settlement and lateral spreading in a gently sloped ground) can be reduced by various ground improvement techniques. Lateral spreading can occur even on very gently sloped ground with an inclined angle as small as 4 -10° relative to the horizontal and can cause tremendous damage to pile foundations.

Several countermeasures against soil liquefaction have been surveyed and evaluated. Yasuda (2005) gave a comprehensive literature review on the countermeasures against soil liquefaction and classified these methods into two categories of ground treatments that prevent soil from liquefaction and strengthen structures to prevent or minimize damage if the ground liquefies. Ground treatments against liquefaction hazards include: (1) in-situ densification, (2) drainage to reduce the generation of excess pore water pressure, (3) solidification, (4) reduction of the degree of saturation to increase the effective stress, and (5) reduction of the magnitude of shear deformations and containment of excess pore water pressure migration.

Each remedial measure provides a degree of effectiveness against liquefaction but has its own limits on construction work; therefore, engineers must select the appropriate countermeasure in accordance with the remedial site conditions. The use of walls to enclose the liquefiable sand offers a method of liquefaction remediation that can be suitable for existing building applications. Okamura and Matsuo (2002), Okamura et al. (2006), Brennan and Madabhushi (2005), and Adalier et al. (2003) performed a series of dynamic centrifuge tests using sheet piles or solidified zones under the toes of earth embankment. They concluded that if a sheet pile enclosure extended into the non-liquefied layer and small gravel berms were added at the embankment toe areas, the cracking, vertical settlement on the embankment, and lateral spreading of the foundation soil were effectively eliminated. Zheng et al. (1996) performed 2-D and 3-D finite element simulations of the countermeasures against liquefaction using a sheet pile ring to model oil tank sites. They concluded that the excess pore water pressure and settlement of the oil tank could be significantly reduced during large earthquakes. Dashti et al. (2010) and Mitrani and Madabhushi (2012) found that rigid containment walls offered very effective methods of liquefaction remediation by restraining lateral sand movement, reducing volume changes in the contained soil, and preventing the in-flow of pore water from the free field. The studies mentioned above focused on liquefaction remediation in level ground by means of walls that enclosed the shallow foundation. No detailed studies have yet investigated the seismic behavior of enclosed walls implemented to reduce the lateral displacements induced by lateral spreading occurred in gently sloped ground.

In Taipei city, an underground conduit was constructed between the Banchia railway station and the Taipei railway station to make way for both the Taiwan railway and the Taiwan high-speed railway systems, thereby reducing the interference of these systems with road traffic. This tunnel was constructed using a cut-and-cover method. Two parallel slurry walls 36 m in depth and 1 m thick were built first, and a bracing system was used to support the surrounding soils during soil excavation to a 17 m deep. Finally, the tunnel was constructed. The completed tunnel was enclosed by two parallel walls, as shown in Figure 1. Because parts of this tunnel route passed through liquefiable soils, the possibility of tunnel uplift and lateral displacement as a result of lateral spreading during earthquakes raised concerns after an upgrade of the design peak ground acceleration (PGA). As a result, it became necessary to re-evaluate the seismic behavior of the liquefiable sand between the parallel walls, as well as the protective effects of the two parallel walls against uplift of tunnel and lateral spreading.

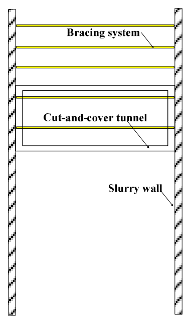

Figure 1 Typical construction section of cut-and-cover tunnel

In situ investigations of liquefaction phenomena are difficult because earthquakes occur infrequently and unpredictably. Without a sufficient number of well-documented case histories describing the effectiveness of a remedial measure, the key parameters that affect soil and structure response must be identified and studied through the careful performance of physical model tests. Small-scale physical modeling provides an alternative to geotechnical earthquake engineering and has been used to gain insights into failure mechanisms. Geotechnical modeling requires the reproduction of the strength and stiffness associated with soil behavior. Soil behavior depends on the stress level and stress history. Centrifuge modeling enables complex scenarios to be reproduced at small scales and at low costs. The use of a soil with a soil density ρ in both a prototype and in a centrifuge model subjected to an inertial acceleration field of N times the earth's gravity yields a vertical stress at a depth h_m (the subscript m denotes the centrifuge model) that is identical to that of the corresponding prototype at a depth h_p (the subscript p denotes the prototype), where $h_p = Nh_m$. The model : prototype scale factor for linear dimensions is 1:N. This relationship is the scaling law of the centrifuge modeling; that is, the stress and pressure similarities are achieved at homologous points. The key scaling relationships for certain dynamic events are listed in Table 1. The scaling relationships were applied to a prototype subjected to base shaking (the amplitude of the base acceleration, a_p, and the frequency, f_p) in the earth's gravity (1 g), such that the corresponding 1/N centrifuge model was tested at an acceleration of Ng and subjected to base shaking (where the amplitude of acceleration is $a_m = Na_p$ and the frequency is $f_m = Nf_p$). The scale factors that retained the stress and pressure similarities of the linear dimensions and base acceleration, a, of the centrifuge model and the prototype were 1:N and 1:N^{-1}, respectively. In most cases it is desirable to use the prototype materials in the model test because it is impossible to find an alternative material (particle size are scaled at a factor of N) with the correct properties. This scale effect on the test results can be verified and discussed by the skill of modeling of models. Fugslang and Ovesen (1988) have found that at least 30 particles must be in contact with each linear dimension of the model structure for the observed behavior to be representative of the prototype behavior.

Table 1 Scaling Relationships of Dynamic Centrifuge Modelling (Schofield, 1980)

Parameter	Prototype	Centrifuge modelling (Ng)
Stress and pressure	1	1
Displacement	1	1/N
Velocity	1	1
Acceleration	1	N
Frequency	1	N
Time (dynamic)	1	1/N
Time (consolidation)	1	1/N^2

This paper focuses on the seismic behavior of a 4° sloped liquefiable sand deposit confined within parallel walls during earthquakes. A series of centrifuge shaking table tests was conducted to investigate the key parameters related to the lateral spreading of soil confined within parallel walls and having various row distances, penetration depths, and with or without a fixed configuration at the base of the parallel walls. All measurements in the paper are presented in prototype units unless specially noted otherwise.

2. GEOTECHNICAL CENTRIFUGE MODELING AND TESTING PROCEDURES

2.1 Testing equipment

The experimental work presented here was undertaken in the Centrifuge at the National Central University (NCU), Taiwan. The NCU Centrifuge has a nominal radius of 3 m and is equipped with a 1-D servo-hydraulically controlled shaker integrated into a swing basket. The shaker has a maximum nominal shaking force of 53.4 kN, a maximum table displacement of ±6.4 mm, and is operated at up to an 80 g centrifugal acceleration. The nominal operating frequency range was 0–250 Hz. A laminar container with inside dimensions of 711 mm x 356 mm x 353 mm was constructed from 38 light-weight aluminium alloy rings arranged in a stack. Each ring was 8.9 mm in height and was separated from the adjacent rings by roller bearings that were specially designed to permit translation in the longitudinal direction with minimal frictional resistance. The laminar container was designed for dry or saturated soil models and permits the development of stresses and strains associated with 1-D wave propagation [Lee et al. 2012]. A flexible 0.3 mm thick latex membrane bag was used to retain the soil and the pore fluid within the laminar container.

2.2 Preparation of the sand bed and fabrication of the parallel wall model

Fine quartz sand was used to prepare the uniform sand deposit. The characteristics of the quartz sand are listed in Table 2. Figure 2 shows the grain size distribution curve of the quartz sand used in the model tests. Two rows of walls manufactured from aluminum plates having two different wall stiffness values (EI) were first fixed at the container. The quartz sand was pluviated along a regular path into the container from a hopper at various falling heights and at a constant flow rate to prepare a fairly uniform sand deposit having a relative density of about 50%. Finally, the saturation process was conducted.

Table 2 Characteristics of Fine Quartz Sand

	G_s	D_{50} in (mm)	D_{10} in (mm)	[1]ρ_{max} (g/cm^3)	[1]ρ_{min} (g/cm^3)
Quartz sand	2.65	0.193	0.147	1.66	1.44

[1]The maximum and minimum densities of the sand were measured in the dry state, according to the method (JSF T 161-1990) specified by the Japanese Geotechnical Society.

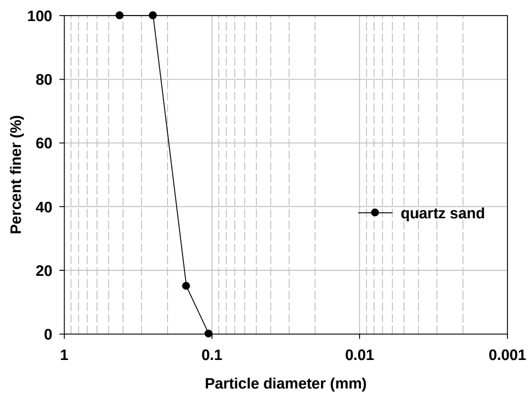

Figure 2 Grain size distribution of quartz sand

A vacuum method was used to ensure saturation of the sand bed. The testing set-up for the saturation of the sand beds is shown in Figure 3. An acrylic plate was used to tightly cover the container during the sand saturation process. Air was then simultaneously and continuously vacuumed out from both the inside and the outside of the container. At the same time de-aired water was carefully dripped by gravity into the container under a vacuum pressure of 80 kPa to saturate the sand bed until the water level extended 2 mm above the sand surface. Overall, one and a half days was needed to saturate the test sand bed. Figure 4 shows the test package resting on the shaker and is ready to perform the centrifuge test.

After saturating the sand bed, the centrifuge was accelerated at 10 *g* per step until it reached an acceleration of 80 *g*. At each step (g-level), the model was allowed to equilibrate for 5 minutes to ensure that the sand bed reached full consolidation at the current overburden stress. Finally, the model was excited using a 1-D sinusoid acceleration consisting of 16 cycles with maximum amplitudes of 0.05 *g* (small shaking events) and 0.21 *g* (large shaking events) and a frequency of 1 Hz in prototype units. The acceleration, pore water pressure, and displacement time histories at different locations were recorded simultaneously.

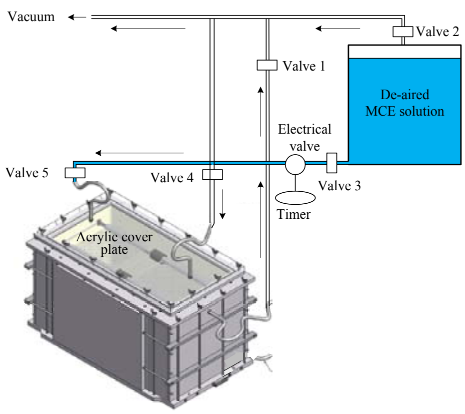

Figure 3 Test setup for saturation of sand model

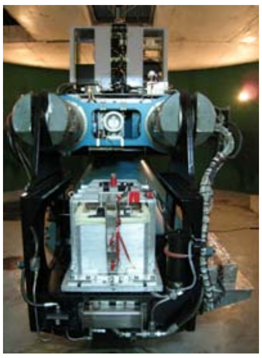

Figure 4 Test package resting on the shaker

2.3 Testing setup and testing conditions

Figures 5(a)-5(f) show schematic diagrams of a laminar container to illustrate the dimensions of the test sand bed, the position of the parallel walls, and the types and positions of the instruments used in the model tests (Stest1–Stest6). The thickness of the model sand bed was 33 cm in the model scale, and the sand bed was inclined by a 4° angle relative to the horizontal. The centrifuge model simulated a 26.4 m thick, 56.8 m long sand deposit in the prototype scale at a centrifuge acceleration of 80 *g*. The sand bed was instrumented with seven vertically spaced accelerometers (A#, PCB type, range ±4905 m/s^2) to record the shear wave propagating from the base to the ground surface in the soil both within and outside of the parallel walls, as shown in Figure 5(a)–5(f). At a given elevation close to the center of the accelerometer array were positioned four pore-water pressure transducers (P#, PDCR81, range 3 bars). Two LVDTs were installed on the surface to measure the time history of the surface settlement within the walls and outside of the walls. Two LVDTs (Schaevitz, range ±10 cm) were positioned at the top of one of the walls to measure the horizontal displacements of the wall. Five LVDTs were attached to the sidewalls of the laminar container to measure the horizontal displacement profile along the depths in the sand deposit.

A sampling rate of 5000 samples/s was used to collect the time histories from all the instrumented transducers through a NI DAQ system. This comprehensive instrumentation set-up and the collection of these detailed measurements were necessary to understand the seismic responses and the associated excess pore water pressure generation at various elevations in a sand deposit confined within parallel walls during 1-D base shaking. A total of six centrifuge shaking table tests were conducted. The test conditions in the prototype for each model are listed in Table 3. Stest1 represents a benchmark test and constituted the uniform sand deposit without parallel walls. Stest2–Stest6 represent the sand deposits confined within the parallel walls and having various penetration depths (*D*), row distances between the walls (*B*), stiffness values of the wall (*EI*), and configuration type (free and fixed) on the wall bottom. The Stest5 and Stest6 conditions held the parallel walls fixed at the container bottom and confined within 3 cm thick cemented sand. Each test was subjected to two events: small base shaking (0.05 g) and large base shaking (0.21 g). The test conditions described in Table 3 were used to study the extent to which lateral spreading induced by liquefaction was mitigated in the sand deposit confined within the parallel walls.

Table 3 Summaries of Test Arrangements and Conditions

Test No.	D_r (%)	Penetration Depth *D* (m)	Row distance *B* (m)	Fixed type	Stiffness of wall (*EI*) MPa-m^4/m
Stest1	50.6	-	-	-	-
Stest2	50.6	10	18	free	23.6
Stest3	54.9	25.6	18	free	23.6
Stest4	52.8	25.6	9	free	23.6
Stest5	49.9	26.4	18	fixed	23.6
Stest6	43.9	26.4	18	fixed	1507

3. TEST RESULTS AND INTERPRETATIONS

3.1 Comparison of time histories of excess pore-water pressure ratio within the parallel walls

3.1.1 Influence of the penetration depth and row distance on the excess pore water pressure generation

The generation and dissipation of excess pore-water pressure in both the level ground and the sloped sand deposit during shaking can lead to the loss of soil stiffness and strength and result in ground deformations and structure settlement. The ratio of the excess pore water pressure, r_u, is a key parameter for evaluating the extent of liquefaction in a sand deposit.

$$r_u = \frac{\Delta u}{\sigma'_{ov}} \quad (1)$$

where Δu is the excess pore water pressure and σ'_{ov} is the effective overburden pressure. Figures 6(a)–6(f) show the time histories of the measured values of r_u at different depths for Stest1 (free field), Stest2 (penetration depth *D*=10 m), and Stest3 (*D*=25.6 m), respectively, during the small base shaking event (0.05 *g*). These figures revealed that no liquefaction occurred over the sand deposit during this small shaking event, although a reduction in r_u was measured at positions between the parallel walls. The deeper the parallel walls penetrated into the sand deposit, the greater the reduction in the values of r_u.

Figures 7(a)–7(f) show the time histories of the measured values of r_u at different depths during the large base shaking (0.21 *g*). These figures also revealed that the parallel walls could reduce the generation of excess pore water pressure. The deeper the parallel walls penetrate into the sand deposit the more effective to reduce the excess pore water pressures generation in the deep layer in both the cases of the small base shaking and the large base shaking event; however, the soil near the surface remained on the verge of liquefaction under large base shaking.

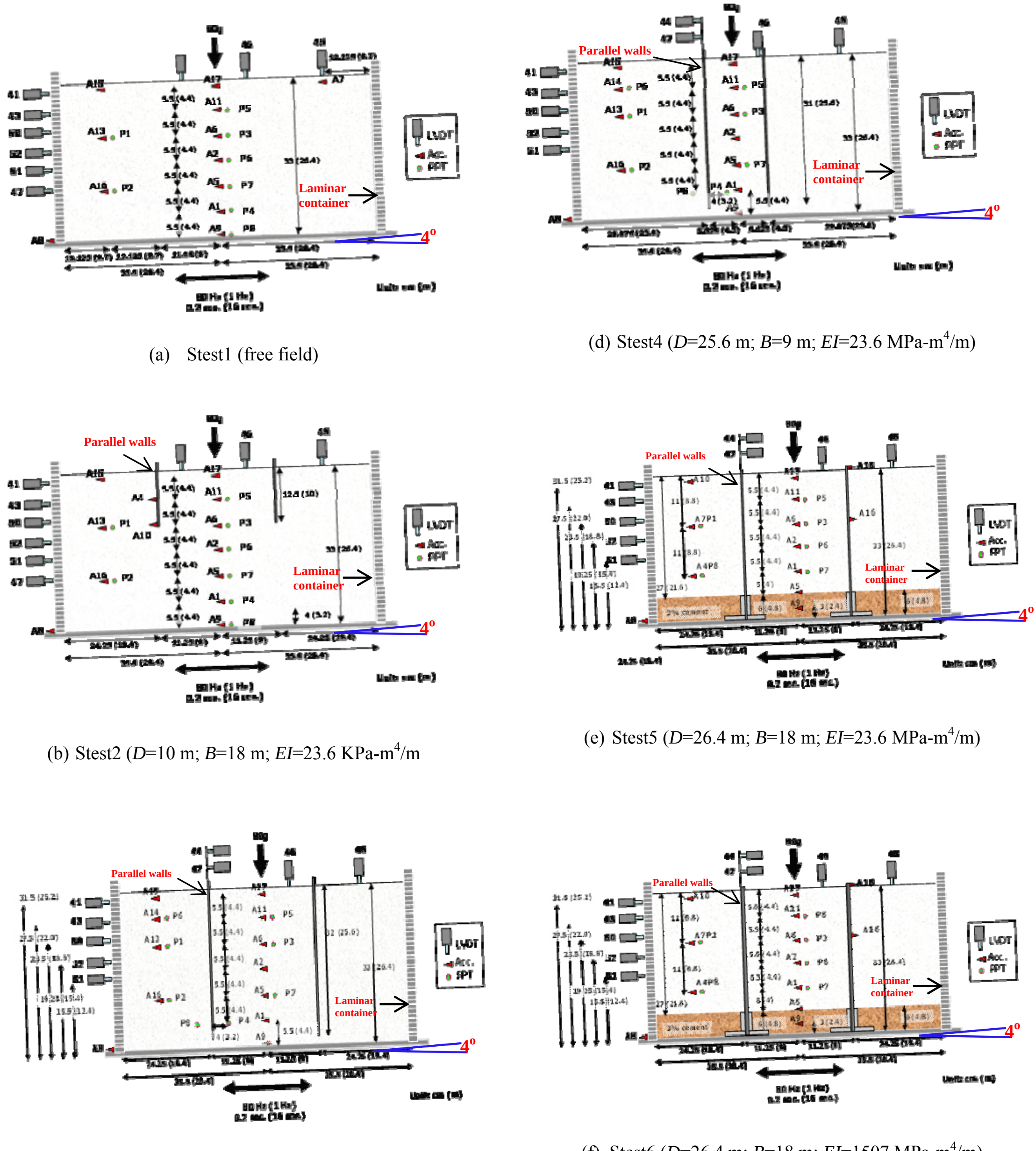

(a) Stest1 (free field)

(d) Stest4 (D=25.6 m; B=9 m; EI=23.6 MPa-m^4/m)

(b) Stest2 (D=10 m; B=18 m; EI=23.6 KPa-m^4/m

(e) Stest5 (D=26.4 m; B=18 m; EI=23.6 MPa-m^4/m)

(c) Stest3 (D=25.6 m; B=18 m; EI=23.6 MPa-m^4/m)

(f) Stest6 (D=26.4 m; B=18 m; EI=1507 MPa-m^4/m)

Figure 5 Soil profile and instrumentations of the models: (a) Stest1; (b) Stest2; (c) Stest3; (d) Stest4; (e) Stest5; (f) Stest6.)
(The model dimensions are in centimetres and prototype dimensions (in parentheses) are in meters.)

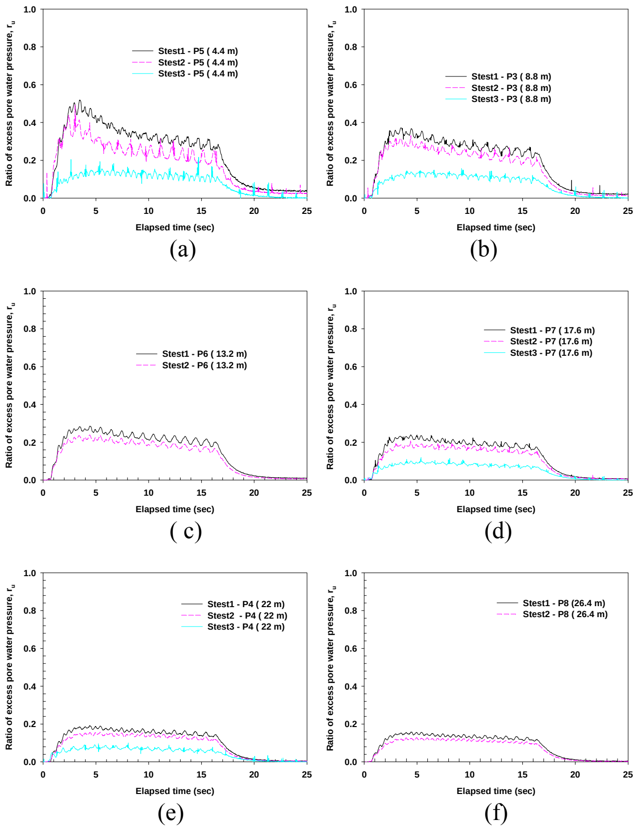

Figure 6 Time histories of ratio of excess pore-water pressure at different depths for Stest1, Stest2 and Stest3 subjected to small base shaking (0.05 g)

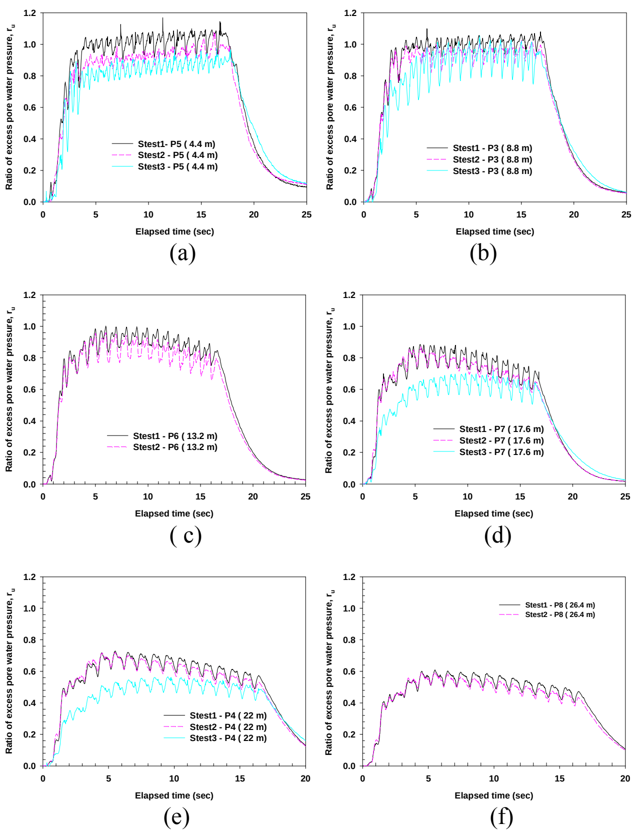

Figure 7 Time histories of ratio of excess pore-water pressure at different depths for Stest1, Stest2 and Stest3 subjected to large base shaking (0.21 g)

Figures 8 and 9 show the time histories of the ratio of excess pore-water pressure at different depths for Stest3 (B = 18 m) and Stest4 (B = 9 m) subjected to the small and large base shaking. An analysis revealed that the parallel walls of small row distance did not reduce the excess pore water pressure generation during either small or large shaking events. The use of the small row distance in the case could not decrease the levels of excess pore-water pressure generation in both the cases of the small and large base shaking. No obvious effect on the reduction of excess pore water pressure is observed for the lower-stiffness parallel walls with small row distance and without fixed the parallel walls at bottom.

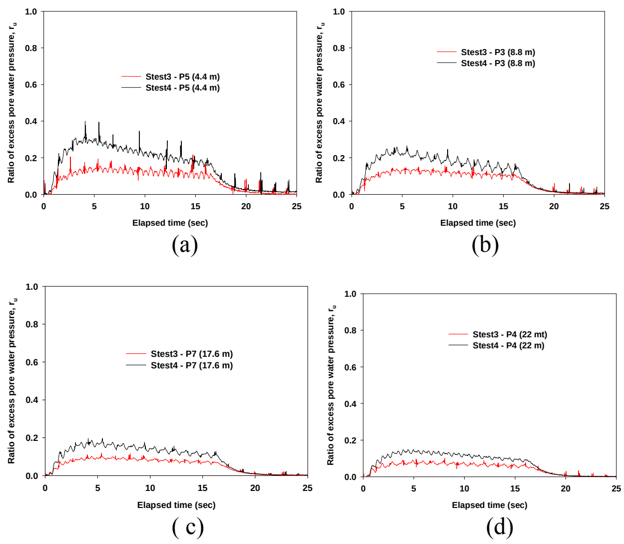

Figure 8 Time histories of ratio of excess pore-water pressure at different depths for Stest3 and Stest4 subjected to small base shaking (0.05 g)

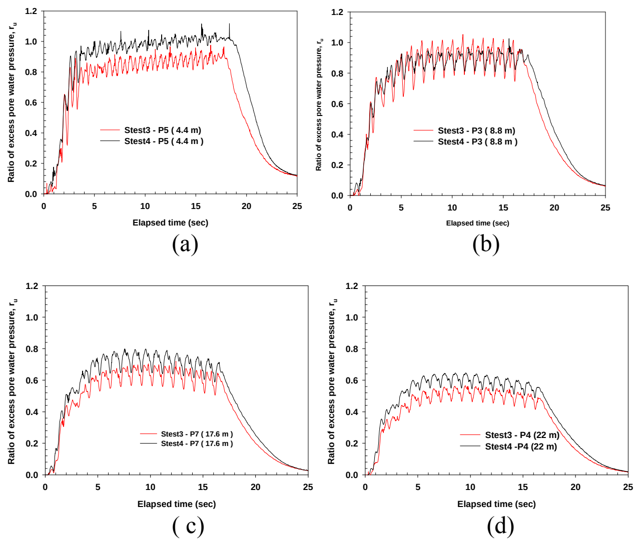

Figure 9 Time histories of ratio of excess pore-water pressure at different depths for Stest3 and Stest4 subjected to large base shaking (0.21 g)

3.1.2 Influence of the wall stiffness for a fixed wall bottom on the excess pore water pressure generation

The slurry wall usually penetrated into the hard layer to retaining the lateral soil and then a cut-and-cover tunnel was constructed. From the design point of view, the fixed end condition appeared somewhere below the excavation level. Accordingly, the parallel walls having two distinct wall stiffness values remained fixed at their bases for Stest5 and Stest6 conditions. Figures 10(a)–10(d) and Figure 11(a)–11(d) show the time histories of r_u measured at different depths for Stest5 (EI=23.6 MPa m^4/m) and Stest6 (EI=1507 MPa m^4/m), which were subjected to the small and large base shaking. The time histories of r_u measured at the corresponding depths for Stest3 are also plotted in Figure 10(a)–10(d) and Figure 11(a)–11(d) for comparison.

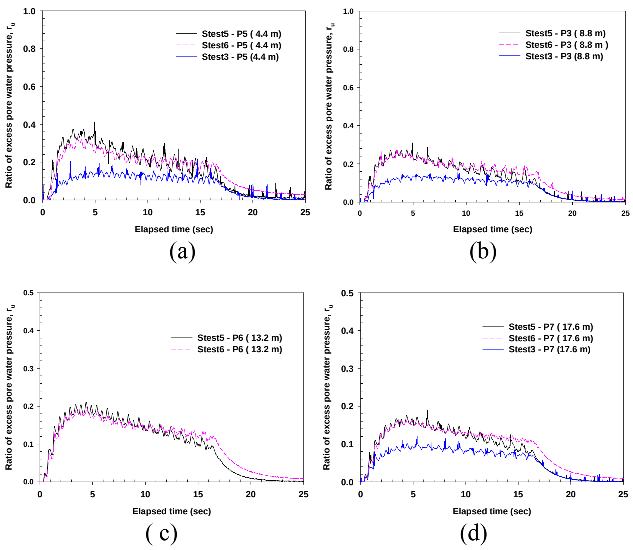

Figure 10 Time histories of ratio of excess pore-water pressure at different depths for Stest5, Stest6 and Stest3 subjected to small base shaking (0.05 g)

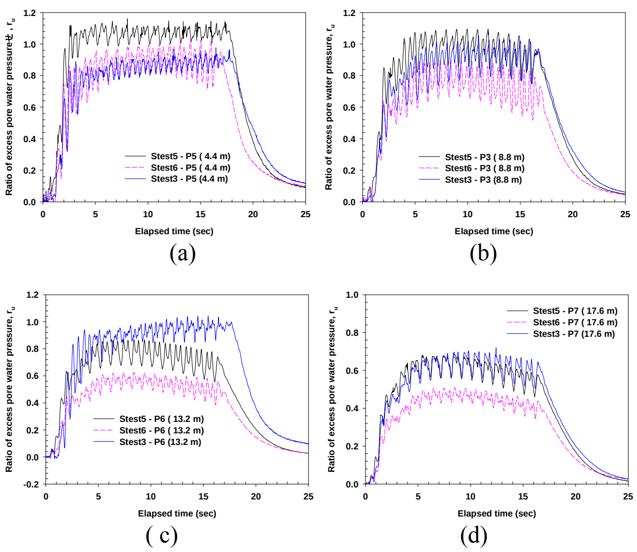

Figure 11 Time histories of ratio of excess pore-water pressure at different depths for Stest5, Stest6 and Stest3 subjected to large base shaking (0.21 g)

The fixed end conditions and high-stiffness parallel walls may more effectively prevent excess pore water pressure generation than the low-stiffness walls do under a large base shaking event; however, no obvious benefits accrued toward preventing excess pore water pressure generation under small base shaking events. As shown in Figure 10(a)–10(d), the sand deposit confined within the parallel walls under fixed end conditions (Stest5 and Stest6) generated a higher excess pore water pressure than those generated in the sand deposit confined within the parallel walls but without fixed end conditions (Stest3), in the presence of small base shaking events. By contrast, the high-stiffness parallel walls reduced the generation of excess pore water pressure in the deeper layers, although the pore water pressure generation in the shallower layer did not effectively decrease under large base shaking events.

3.2 Comparison of time histories of acceleration measured at different depths within the parallel walls

Figure 12 shows the time histories of acceleration measured at various depths in the free field sand deposit (Stest1) and in the sand deposit confined within the parallel walls (Stest2, Stest3, Stest4, Stest5, and Stest6), subjected to small base shaking events. The accelerations in the sand deposits confined by the fixed end parallel walls displayed only slightly larger amplitudes than the accelerations measured in the free field or in a sand deposit confined within free end parallel walls. The embedded parallel walls only appear to slightly affect the seismic responses of the sand bed during small shaking events. No negative down-slope accelerations were observed in these tests.

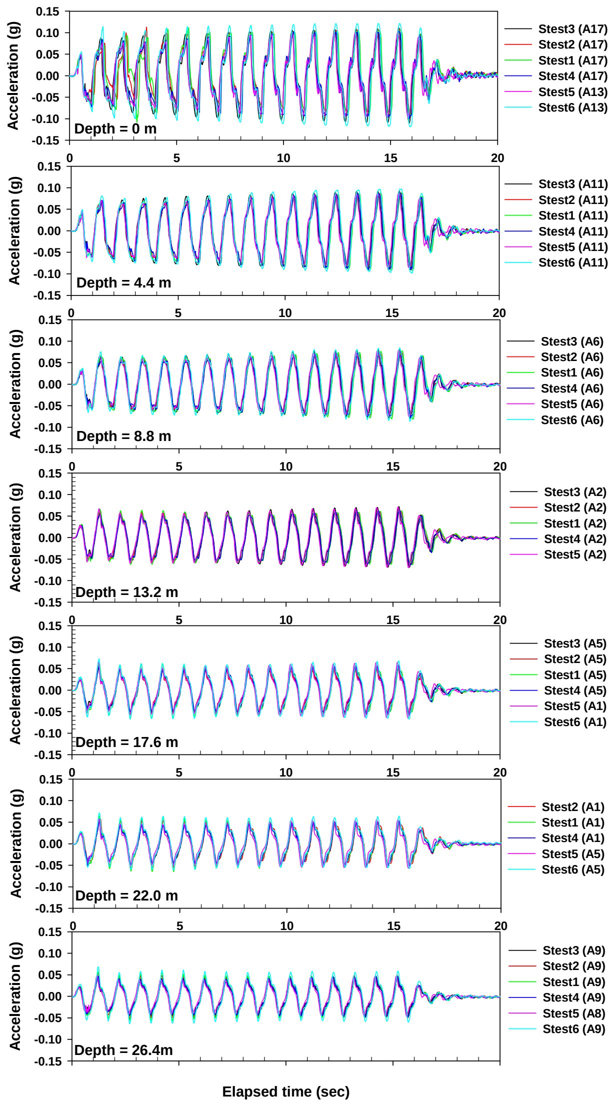

Figure 12 Time histories of acceleration at different depths for Stest1, Stest2, Stest3, Stest4, Stest5, Stest6 subjected to small base shaking (0.05 g)

Figure 13 shows the time histories of acceleration measured at various depths in the free field sand deposit (Stest1) and in the sand deposit confined within the free end parallel walls (Stest2 and Stest3, B=18 m) and subjected to large base shaking. As shown in Figure 13, the parallel walls with deeper penetration depths were correlated with smaller amplitude down-slope accelerations (negative accelerations) at the depth of 8.8 m. The parallel walls can slightly reduce the magnitudes of the acceleration, shear stresses, and generation of excess pore water pressure in the sand deposit within the parallel walls, as shown in Figure 7. Figure 14 shows the time histories of the acceleration at different depths for Stest3 (row distance B= 18 m) and Stest4 (B= 9 m) subjected to a large base shaking event (0.21g). The row distance between the free end and lower stiffness parallel walls can decrease the seismic responses of the soil within the walls to only a small degree because the amplitudes of the measured accelerations along the depths did not differ significantly in these two tests.

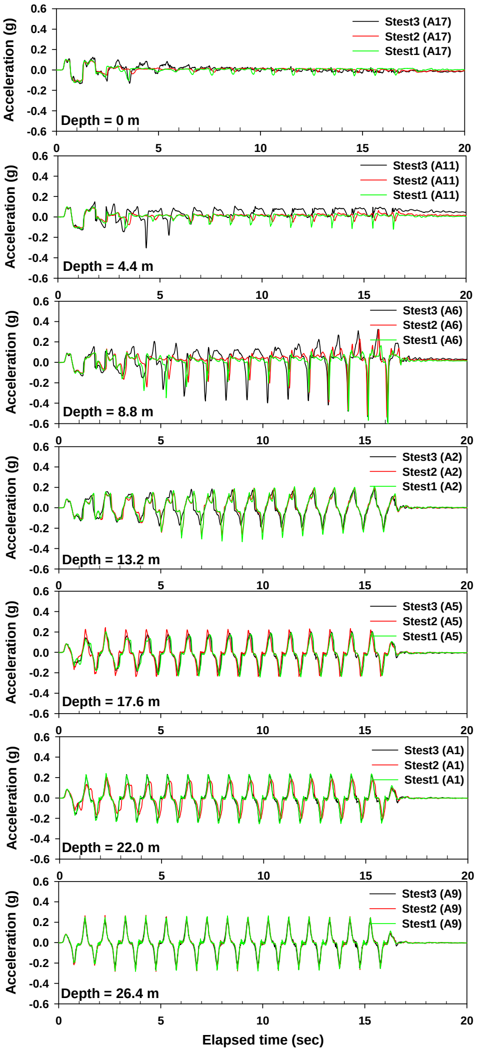

Figure 13 Time histories of acceleration at different depths for Stest1, Stest2 and Stest3 subjected to large base shaking (0.21 g)

Figure 15 shows the time histories of the acceleration measured at different depths for Stest3 (EI=23.6 MPa m^4/m, B=18 m, free end on the bottom), Stest5 (EI=23.6 MPa m^4/m, B=18 m, fixed end at the bottom), and Stest6 (EI=1507 MPa m^4/m, B=18 m, fixed end at the bottom) subjected to large base shaking. Positive and negative sharp spikes were observed in the acceleration records measured at the depth of 8.8 m for Stest5 or at the depth of 4.4 m in Stest6. The positive and negative acceleration spikes measured in Stest6 were more symmetrical than those measured in Stest5. The depths of the sharp spikes become shallower with the use of stiffer parallel walls (Stest6). The fixed end parallel walls contributed to the propagation of shear waves directly from the base into the soil between the parallel walls and introduced large accelerations into the top of the sand deposit between the parallel walls.

Figures 16(a) and 16(b) illustrate the time histories of the accelerations measured at the tops of the walls in Stest5 and Stest6. The accelerations measured at the surfaces of the sand deposit, as shown in Figure 14 and 15, were smaller than those measured at the walls, as shown in Figure 16. The walls itself directly experienced and propagated the large accelerations from the base to the surface, especially in the case of low-stiffness parallel walls. Consequently, protected structures should not be connected with the surrounding parallel walls to avoid transmitting the large accelerations experienced by the parallel walls.

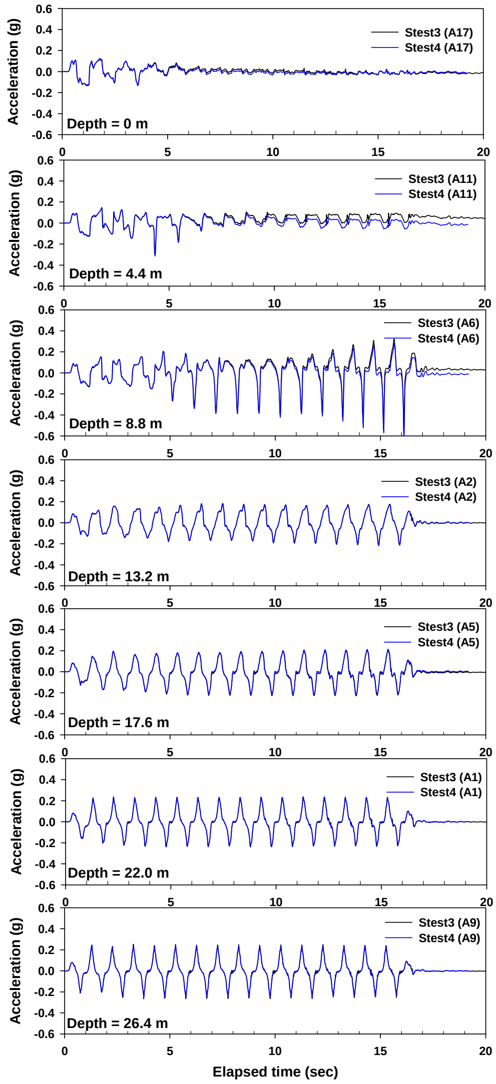

Figure 14 Time histories of acceleration at different depths for Stest3 (B=18 m) and Stest4 (B=9 m) subjected to large base shaking (0.21 g)

3.3 Comparison of the horizontal displacements of laminar container and parallel wall

Lateral spreading induced by liquefaction produced down-slope horizontal displacements, as shown in Figure 17, in Stest1 (free field). These horizontal displacements were measured at different depths on the sidewall of the laminar container, as shown in Figure 5. The negative displacements represent the down-slope displacements. The permanent down-slope displacement reached 0.61 m on the surface of the free field sand deposit. Permanent lateral ground displacements due to lateral spreading in a free field may induce huge disaster to geotechnical structures (Ishihara et al. 1996).

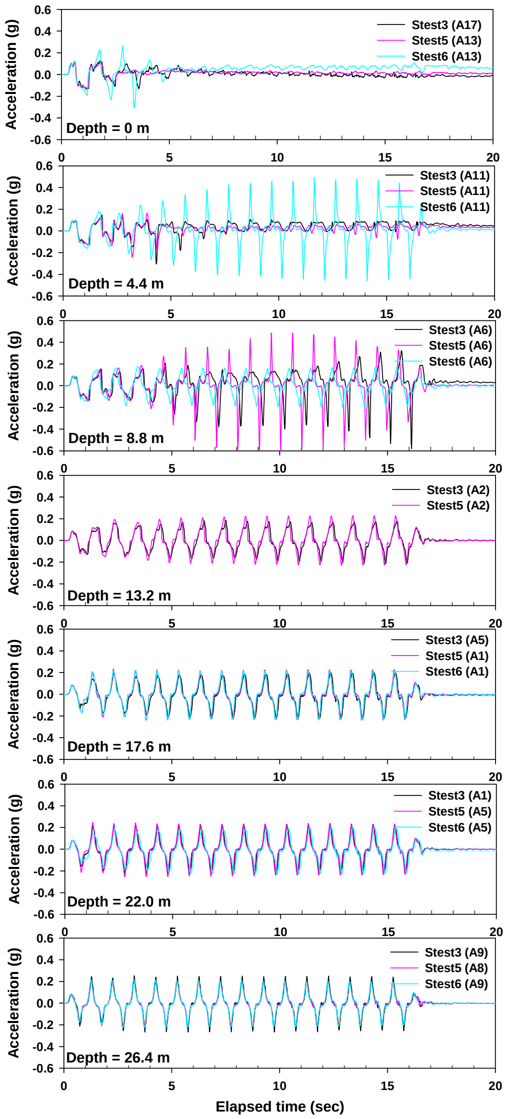

Figure 15 Time histories of acceleration at different depths for Stest3, Stest5 and Stest6 subjected to large base shaking (0.21 g)

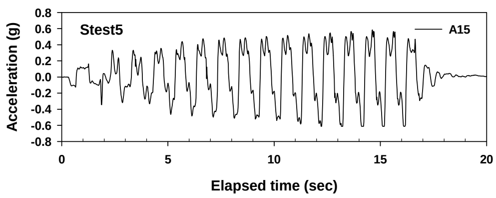

(a)

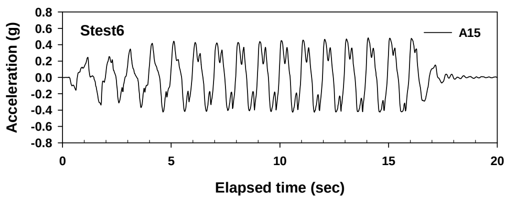

(b)

Figure 16 Time histories of acceleration at the top of parallel walls (a) Stest5; (b) Stest6 subjected to large base shaking (0.21 g)

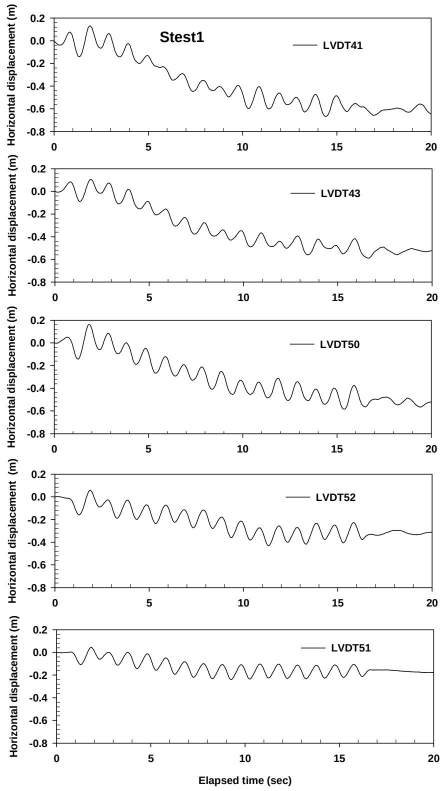

Figure 17 Time histories of horizontal displacement measured at different depths on the laminar container for Stest1 subjected to large base shaking (0.21 g)

Figures 18(a)–18(d) show the time histories of the horizontal displacements measured at the tops of the parallel walls for Stest3, Stest4, Stest5, and Stest6. The end conditions of the parallel walls (free or fixed at the bottom of the wall) did not affect the large 0.4–0.5 m permanent horizontal displacements observed in the presence of low-stiffness parallel walls, as shown in Figure 18(a), 18(b), and 18(c), under large shaking events. Low-stiffness parallel walls did not appear to effectively reduce the magnitude of permanent horizontal displacements within the parallel wall and thereby the structures were not protected from the damages caused by lateral spreading. By contrast, the parallel walls with a large stiffness (EI=1507 MPa m^4/m) and a fixed wall base can effectively reduce the permanent horizontal wall displacements to less than 0.06 m, as shown in Figure 18(d). Hence only use of high-stiffness parallel walls can prevent the structures within the walls from the damages resulted from the lateral spreading during large earthquakes.

3.4 Comparison of the time histories of the surface settlements within the parallel walls

Figures 19(a) and 19(b) show the time histories of the surface settlements measured at positions within the parallel walls under small shaking events and large shaking events, respectively. The free field sand deposit, which was not confined within the parallel walls, experienced the largest surface settlement under both the small and large shaking events. The parallel walls that penetrated to a deeper depth produced smaller surface settlements. The use of high-stiffness parallel walls with fixed ends in the non-liquefied deposits can more effectively reduce the surface settlement of the liquefiable sand deposit between the parallel walls during base shaking. The reduction of the settlements to the ground surface can effectively decrease the impacts on buildings, pile foundations. These would be benefit to minimize the damages if ground liquefied.

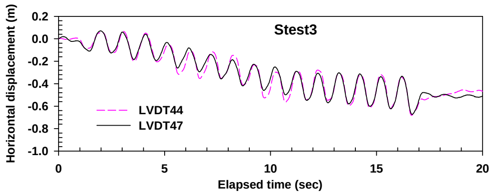

(a)

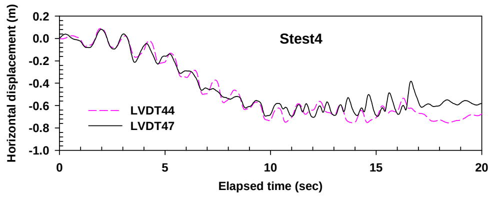

(b)

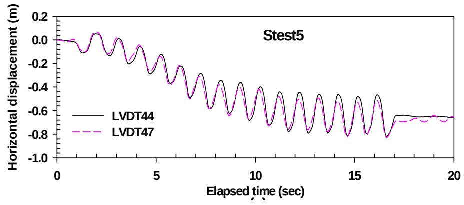

(c)

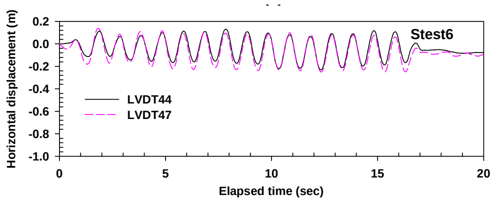

(d)

Figure 18 Time histories of the measured horizontal wall displacement in the cases of different end fixed conditions and different stiffness of wall subjected to large base shaking (0.21 *g*): (a) Stest3; (b)Stest4; (c)Stest5; (d)Stest6.

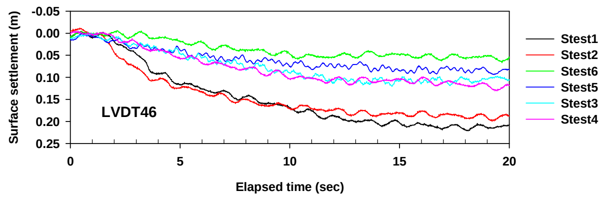

(a)

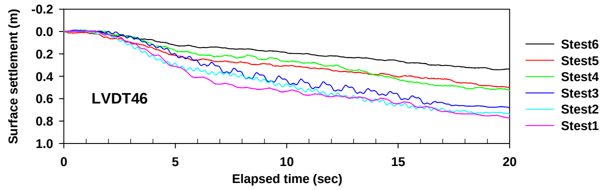

(b)

Figure 19 Time histories of the surface settlement for Stest1, Stest2, Stest3, Stest4, Stest5, and Stest6 ; (a)small shaking event (0.05 *g*); (b) large shaking event (0.21 *g*).

4. CONCLUSION

A series of 1-*D* centrifuge shaking table tests under an acceleration of 80 *g* was performed to investigate the seismic behavior of a 4° degree sloped liquefiable sand deposit confined within parallel walls, having various depths and row distances, and with different fixed bases. The test results showed that parallel walls could relieve the build-up of excess pore-water pressure within the deeper sand layer, although the excess pore-water pressure in the shallower sand layer did not decrease significantly during large base shaking. Parallel walls with an appropriate drainage system may be necessary to effectively reduce the excess pore water pressure generation. The effectiveness at decreasing surface settlement between walls increased with the penetration depth and bending stiffness of the wall. High-stiffness parallel walls with fixed ends constrained the enclosed sands effectively and prevented lateral displacements resulting from the liquefaction-induced lateral spreading; however, the walls experienced and propagated large accelerations to the surrounding soils. Protected structures should not be connected with parallel walls to avoid introducing large accelerations.

5. REFERENCES

Abdoun, T., Dobry, R., Zimmie, T.F., and Zeghal, M. (2005) "Centrifuge Research of Countermeasures to Protect Pile Foundations Against Liquefaction-induced Lateral Spreading". Journal of Earthquake Engineering, 9(1), pp105-125.

Adalier K., Pamuk, A., Zimmie, T.F. (2003) "Seismic Rehabilitation of Coastal Dikes by Sheet-pile Enclosure". Proceeding of the 13th International Offshore and Polar Engineering Conference, pp474-480.

Brennan, A.J. and Madabhushi, S.P.G. (2005) "Liquefaction and Drainage in Stratified soil". Journal of Geotechnical and Geoenviromental Engineering, 131(7), pp876-885.

Dashti, S., Bray, J.D., Pestana, J.M., Riemer, M., Wilson, D. (2010) "Centrifuge Testing to Evaluate and Mitigate Liquefaction-induced Building Settlement Mechanism". Journal of Geotechnical and Geoenviromental Engineering 136(7), pp918-929.

Fuglsang, L.D., Ovesen, N.K. "The Applicationof the Theory of Modeling to Centrifuge Studies", In Centrifuges in Soil Mechanics (eds Craig, W.H., James, R.G., Schofield, A.N.), pp119-138.

Ishihara K, Yasuda S, Nagase H. (1996) "Soil Characteristic and Ground Damage". Soils and Foundations special issue on geotechnical aspects of the January 17 1995 Hyogoken-Nambu earthquake: Japanese Geotechnical Society, pp109-118.

Lee, C.J. (2005) "Centrifuge modeling of the behavior of caisson-type quay walls during earthquake". Soil Dynamics and Earthquake Engineering, 25(2), pp117-131.

Lee, C.J., Wei, Y.C., and Kou, Y.C. (2012) "Boundary Effects of a Laminar Container in Centrifuge Shaking Table Tests". Soil Dynamics and Earthquake Engineering, 34(1), pp37-51.

Mitrani, H., Madabhushi, S.P.G. (2012) "Rigid containment walls for liquefaction remediation". Journal of Earthquake and Tsunami, 6(4), pp1250017-1250023.

Okamura, M., Masuo, O. (2002) "Effects of Remedial Measures for Mitigating Embankment Settlement due to Foundation Liquefaction," International Journal of Physical Modeling in Geotechnics, 2(2), pp1-12.

Okamura, M., Ishihara, M. Tamura, K. (2006) "Liquefied Soil Pressures on Vertical Walls with Adjacent Embankments". Soil Dynamics and Earthquake, 26(3), pp 265-274.

Schofield, A.N. (1980) "Cambridge geotechnical centrifuge operations". Geotechnique, 30(3), pp227-268.

Yasuda, S. (2005) "Survey of Recent Remediation Techniques in Japan, and Future Applications". Journal of Earthquake Engineering, 9(1), pp151-186.

Zheng, J., Suzuki, K., Ohbo, N. and Prevost, J.H. (1996) "Evaluation of Sheet Pile-ring Countermeasure Against Liquefaction for Oil Tank Site". Soil Dynamics and Earthquake Engineering, 15(6), pp369-379.